Onset of Relativistic Jet Activity from the Tidal Disruption of a Star by a Massive Black Hole

D. N. Burrows[1], J. A. Kennea[1], G. Ghisellini[2], V. Mangano[3], B. Zhang[4], K. L. Page[5], M. Eracleous[1], P. Romano[3], T. Sakamoto[6,7], A. D. Falcone[1], J. P. Osborne[5], S. Campana[2], A. P. Beardmore[5], A. A. Breeveld[8], M. M. Chester[1], R. Corbet[6,7], S. Covino[2], J. R. Cummings[6,7], P. D'Avanzo[2], V. D'Elia[9], P. Esposito[10], P. A. Evans[5], D. Fugazza[2], J. M. Gelbord[1], K. Hiroi[11], S. T. Holland[6,12], K. Y. Huang[13], M. Im[14], G. Israel[15], Y. Jeon[14], Y.-B. Jeon[16], H. D. Jun[14], N. Kawai[17,20], J. H. Kim[14], H. A. Krimm[6,12], F. E. Marshall[21], P. Mészáros[1], H. Negoro[18], N. Omodei[19], W.-K. Park[14], J. S. Perkins[6,7], M. Sugizaki[20], H.-I. Sung[16], G. Tagliaferri[2], E. Troja[21,22], Y. Ueda[11], Y. Urata[23], R. Usui[17], L. A. Antonelli[15,9], S. D. Barthelmy[21], G. Cusumano[3], P. Giommi[9], A. Melandri[2], M. Perri[9], J. L. Racusin[21], B. Sbarufatti[3], M. H. Siegel[1], & N. Gehrels[21]

[1]*Department of Astronomy & Astrophysics, The Pennsylvania State University, 525 Davey Laboratory, University Park, PA 16802, USA*

[2]*INAF – Osservatorio Astronomico di Brera, Via Bianchi 46, 23807 Merate, Italy*

[3]*INAF – Istituto di Astrofisica Spaziale e Fisica Cosmica, Via U. La Malfa 153, I-90146 Palermo, Italy*

[4]*Department of Physics and Astronomy, University of Nevada, Las Vegas, NV 89154, USA*

[5]*Department of Physics and Astronomy, University of Leicester, University Road, LE1 7RH Leicester, UK*

[6]*CRESST and NASA/GSFC, Greenbelt, MD 20771, USA.*

[7]*University of Maryland, Baltimore County, 1000 Hilltop Circle, Baltimore, MD 21250, USA*

[8]*University College London / Mullard Space Science Laboratory*

[9]*ASI Science Data Center, via Galileo Galilei, 00044 Frascati, Italy*

[10]*INAF – Osservatorio Astronomico di Cagliari, località Poggio dei Pini, strada 54, I-09012 Capoterra, Italy*

[11]*Department of Astronomy, Kyoto University, Oiwake-cho, Sakyo-ku, Kyoto 606-8502, Japan*

[12]*Universities Space Research Association, 10211 Wincopin Circle, Suite 500, Columbia, MD 21044-3432, USA*

[13]*Academia Sinica Institute of Astronomy and Astrophysics, Taipei 106, Taiwan*

[14]*Center for the Exploration of the Origin of the Universe, Department of Physics & Astronomy, FPRD, Seoul National University, Shillim-dong, San 56-1, Kwanak-gu, Seoul, Republic of Korea*

[15]*INAF – Osservatorio Astronomico di Roma, via Frascati 33, I-00040 Monteporzio Catone, Italy*

[16]*Korea Astronomy and Space Science Institute (KASI), 776 Daedeokdae-ro, Yuseong-gu, Daejeon 305-348, Korea*

[17]*Department of Physics, Tokyo Institute of Technology, 2-12-1 Ookayama, Meguro-ku, Tokyo 152-8551, Japan*

[18]*Department of Physics, Nihon University, 1-8-14 Kanda-Surugadai, Chiyoda-ku, Tokyo 101-8308, Japan*

[19]*W. W. Hansen Experimental Physics Laboratory, Kavli Institute for Particle Astrophysics and Cosmology, Department of Physics and SLAC National Accelerator Laboratory, Stanford University, Stanford, CA 94305, USA*

[20]*MAXI team, RIKEN, 2-1 Hirosawa, Wako, Saitama 351-0198*

[21] *NASA Goddard Space Flight Center, Greenbelt, MD 20771, USA*

[22] *Oak Ridge Associated Universities*

[23] *Institute of Astronomy, National Central University, Chung-Li 32054, Taiwan*

Supermassive black holes have powerful gravitational fields with strong gradients that can destroy stars that get too close[1,2], producing a bright flare in UV and X-ray light from stellar debris that forms an accretion disk around the black hole[3–7]. The aftermath of this process may have been seen several times over the past two decades in the form of sparsely sampled, slowly fading emission from distant galaxies[8–14], but the onset of the stellar disruption event has never before been observed. Here we report on observations of a bright X-ray flare from the new extragalactic transient, Swift J164449.3+573451. This source increased in brightness in the X-ray band by a factor of at least 10^4 since 1990 and by a factor of at least 100 since early 2010. Our optical and X-ray observations show that we have captured the onset of relativistic jet activity from a supermassive black hole for the first time. A companion paper[15] comes to similar conclusions based on radio observations. This event is likely due to the tidal disruption of a star falling into a supermassive black hole, but the detailed behaviour differs from current theoretical models of tidal disruption events, showing new signatures associated with the onset of the powerful jet.

Swift J164449.3+573451 (hereafter Sw J1644+57) was discovered when it triggered the *Swift*[16] Burst Alert Telescope[17] (BAT) on 28 March 2011. Subsequent analysis of BAT data taken before the on-board trigger shows that the outburst was first detected on 25 March 2011 (Supplementary Figure 1). The *Swift* X-Ray Telescope[18] (XRT) measured a source position[19,20] of RA

(J2000): $16^{\rm h}\ 44^{\rm m}\ 49.92^{\rm s}$, Dec (J2000): $+57^\circ\ 35'\ 00.6''$, with a 90% confidence error circle radius of 1.4 arcseconds. Subsequent optical[21] and radio[15] observations showed that a variable radio source was located at the centre of a galaxy within the XRT error circle. Optical spectroscopy[21] measured a redshift of 0.354, corresponding to a luminosity distance of 5.8×10^{27} cm.

We performed broad-band followup observations using γ-ray, X-ray, UV, optical, and near-IR (NIR) telescopes. The flares seen by the BAT are closely tracked with better sensitivity in the 0.3-10 keV band by the XRT (Figure 1). The X-ray light curve is complex and highly variable, with peak isotropic luminosities exceeding 10^{48} erg s^{-1} (Figure 2), implying accretion onto a compact object. The integrated isotropic X-ray power (over the 50 days following the first BAT trigger) is $\sim 2 \times 10^{53}$ erg (1–10 keV). We have found no statistically significant periodic or quasi-periodic signals in the XRT data. Details of our observations and data analysis are given in Supplementary Information section 1.

Sw J1644+57 has not been previously detected at any wavelength and is not present in any sky catalogs. X-ray flux upper limits from observations by *ROSAT, XMM-Newton, MAXI,* and *Swift* between 1990 and 24 March 2011 are 2–4 orders of magnitude lower than the peak X-ray fluxes measured by *Swift* (Figure 2), and the *ROSAT* upper limits are an order of magnitude below the lowest flux in the first 50 days after the first BAT trigger.

Sw J1644+57 is unlike any previously discovered extragalactic X-ray transient. Gamma-ray bursts reach similar peak fluxes and luminosities, but fade much more rapidly and smoothly than Sw J1644+57. The broad class of AGNs cover the range of luminosities that we measured for Sw J1644+57 (3×10^{45} to 3×10^{48} erg s^{-1}), but no individual AGN has been observed to vary by more than about two orders of magnitude. Supernovae have much lower luminosities ($L_x < 3 \times 10^{41}$ erg s^{-1}). Some Galactic transients (such as Supergiant Fast X-ray Transients) vary by similar amounts[22], but their luminosities are 10 orders of magnitude lower than Sw J1644+57. This source appears to be without precedent in its high energy properties.

Our X-ray and NIR observations provide limits on the mass of the accreting black hole. The most rapid observed variability is a 3σ doubling in X-ray brightness over a time scale of $\delta t_{\rm obs} \sim 100$ s. This constrains the size of the black hole under the assumption that the central engine dominates the variability. For a Schwarzschild black hole with mass $M_{\rm bh}$ and radius r_s, the minimum variability time scale in its rest frame is $\delta t_{\rm min} \sim r_s/c \sim 10.0(M_6)$ s, where $M_6 \equiv (M_{bh}/10^6\ \mathrm{M}_\odot)$. At $z = 0.354$, this gives

$$M_{\rm bh} \sim 7.4 \times 10^6 \left(\frac{\delta t_{\rm obs}}{100\ s}\right)\ \mathrm{M}_\odot\ . \tag{1}$$

Much smaller masses are unlikely, as they would lead to shorter timescale variability. However, short time-scale variability can also be produced in a jet with substructure, in which case this constraint may underestimate the black hole mass. We obtain an independent constraint on the black hole mass from the $M_{\rm bh} - L_{\rm bulge}$ relation, which gives an upper limit of $\sim 2 \times 10^7\ \mathrm{M}_\odot$ (see Supplementary Information section 2.1 for details). We conclude that the black hole mass is likely in the range $1 < M_6 < 20$.

For a black hole of this size, the peak isotropic X-ray luminosity exceeds the Eddington luminosity, $L_{\rm Edd} = 1.3 \times 10^{44}\ M_6$ erg s^{-1}, by several orders of magnitude. If the radiation were truly isotropic, radiation pressure would halt accretion and the source would turn off. This contradiction provides strong evidence that the radiation pattern must be highly anisotropic, with a relativistic jet pointed towards us.

In addition to the X-ray observations discussed above, we obtained photometry in the uvw2, uvm2, uvw1, u, b, v, R, J, H, and Ks bands with the *Swift* UVOT, LOAO, BOAO, TNG, UKIRT, CFHT, and Maidanak Observatory telescopes (Supplementary Figure 5). We used our broad-band data set to construct spectral energy distributions (SEDs) at several key time periods in order to constrain models of the emission mechanism (Figure 3). The SEDs show that the broad-band energy spectrum is dominated by the X-ray band, which accounts for 50% of the total bolometric energy output in the high/flaring X-ray state. The optical counterpart of the transient X-ray source is not detected in optical or UV bands, but is detected strongly in the NIR, indicating substantial extinction by dust in the host galaxy. We measure an extinction of $A_V \sim 4.5$ (Supplementary Information section 1.2.3), which corresponds to a neutral hydrogen column density of $\mathrm{N_H} \sim 1 \times 10^{22}$ cm^{-2} for the Galactic ISM gas-to-dust ratio[23]; this is in rough agreement with the measured intrinsic X-ray absorption (Supplementary Figure 11).

The SED constrains the possible emission mechanism. We assume that the NIR and X-ray photons originate in the same emission region, an assumption that is consistent with the NIR and X-ray spectral slopes. The optical-to-X-ray slope then requires a magnetically-dominated, particle-starved jet. Although not shown here, we interpret the radio emission[15] as an external shock in the gas surrounding Sw J1644+57. Details of our modeling are given in the Supplementary

Information sections 2.3 – 2.7.

This luminous, relativistic jet is likely powered by the tidal disruption of a star, which can explain the increase by four orders of magnitude in the X-ray flux from this supermassive black hole, the slow decay in flux following the initial outbursts, and the inferred mass accretion amounting to a substantial fraction of a solar mass (Supplementary Information section 2.2). It is not surprising for such an event to produce an X-ray jet[6,24]. If the accretion is powered by the tidal disruption of a star, we can estimate the jet beaming factor based on the expected statistics of tidal disruption events (TDEs). The *Swift* BAT, with a field of view of $\sim 4\pi/7$ sr and a duty cycle of $\sim 75\%$, has detected one such event in ~ 6 years at a peak flux that would have been detectable to $z \sim 0.8$. The all-sky rate of Sw J1644+57-like events is therefore $R_{4\pi} \sim 1$ yr^{-1}, with a 90% confidence interval[25] of $0.08 - 3.9$ yr^{-1}. Taking into account the volume rate of TDEs and the galaxy number density, and assuming that $\sim 10\%$ of TDEs produce relativistic jets, we estimate that the fraction of TDEs with jets pointed towards us must be $\sim 10^{-3}$ (Supplementary Information section 2.9.1; a similar conclusion was obtained by the companion paper[15]). This jet solid angle can be achieved by a bulk Lorentz factor of $\Gamma \sim 10 - 20$ or a jet opening angle of $\theta_j \sim 5^\circ$.

Our observations of Sw J1644+57 provide a unique data set for studying the onset of jet activity from a supermassive black hole, and are consistent with a prediction that a low-density, magnetically-dominated jet might be formed during the super-Eddington phase of a tidal disruption event[6]. However, little theoretical work has been published discussing observational signatures of the onset of such a jet. Instead, tidal disruption models have concentrated on emission from the stellar surface, the accretion disk, and the surrounding medium: an X-ray or γ-ray thermal flare is expected from the surface of the star as it is crushed by the strong gravitational gradient of the black hole[5,7], with peak luminosity of $< 10^{44}$ erg s^{-1} and a duration of tens of seconds; a phase of super-Eddington accretion of bound debris, accompanied by a wind that interacts with the surrounding medium[6,26], will radiate in the UV–NIR[6] or X-ray[26] bands with luminosity $\lesssim 10^{44}$ erg s^{-1}; and at late times the bolometric luminosity from the accretion disk may undergo a steady decline that traces the rate of return of post-disruption debris[2,27,28], with $\dot{M} \propto (t - t_0)^{-5/3}$. Detailed multi-band light curve models of emission from the accretion disk in TDEs suggest that the X-ray emission should be characterized by a broad, smooth X-ray lightcurve peaking at $L_x \sim 3 \times 10^{44}$ erg s^{-1} weeks to months after the stellar disruption for a $10^6 - 10^7$ $\mathrm{M}_\odot$ black hole[26], in sharp contrast to our observations. The dramatic differences between these model predictions and our observations are likely due to the bright jet in Sw J1644+57, which dominates the much fainter emission from the wind and disk. Long-term monitoring of Sw J1644+57 will help to distinguish between competing models of this event, and will show whether emission from the jet follows the expected $t^{-5/3}$ decay of the mass accretion rate from fallback of stellar debris.

1. Rees, M. J. Tidal disruption of stars by black holes of 10 to the 6th-10 to the 8th solar masses in nearby galaxies. *Nature* **333**, 523–528 (1988).

2. Evans, C. R. & Kochanek, C. S. The tidal disruption of a star by a massive black hole. *Astrophys. J. (Letters)* **346**, L13–L16 (1989).

3. Ulmer, A. Flares from the Tidal Disruption of Stars by Massive Black Holes. *Astrophys. J.*

514, 180–187 (1999).

4. Bogdanović, T., Eracleous, M., Mahadevan, S., Sigurdsson, S. & Laguna, P. Tidal Disruption of a Star by a Black Hole: Observational Signature. *Astrophys. J.* **610**, 707–721 (2004).

5. Guillochon, J., Ramirez-Ruiz, E., Rosswog, S. & Kasen, D. Three-dimensional Simulations of Tidally Disrupted Solar-type Stars and the Observational Signatures of Shock Breakout. *Astrophys. J.* **705**, 844–853 (2009).

6. Strubbe, L. E. & Quataert, E. Optical flares from the tidal disruption of stars by massive black holes. *Mon. Not. R. Astron. Soc.* **400**, 2070–2084 (2009).

7. Brassart, M. & Luminet, J. Relativistic tidal compressions of a star by a massive black hole. *Astron. Astrophys.* **511**, A80 (2010).

8. Brandt, W. N., Pounds, K. A. & Fink, H. The unusual X-ray and optical properties of the ultrasoft active galactic nucleus Zwicky 159.034 (RE J1237+264). *Mon. Not. R. Astron. Soc.* **273**, L47–L52 (1995).

9. Komossa, S. & Bade, N. The giant X-ray outbursts in NGC 5905 and IC 3599:() hfill Follow-up observations and outburst scenarios. *Astron. Astrophys.* **343**, 775–787 (1999).

10. Donley, J. L., Brandt, W. N., Eracleous, M. & Boller, T. Large-Amplitude X-Ray Outbursts from Galactic Nuclei: A Systematic Survey using ROSAT Archival Data. *Astron. J.* **124**, 1308–1321 (2002).

11. Esquej, P. *et al.* Candidate tidal disruption events from the XMM-Newton slew survey. *Astron. Astrophys.* **462**, L49–L52 (2007).

12. Gezari, S. *et al.* UV/Optical Detections of Candidate Tidal Disruption Events by GALEX and CFHTLS. *Astrophys. J.* **676**, 944–969 (2008).

13. Gezari, S. *et al.* Luminous Thermal Flares from Quiescent Supermassive Black Holes. *Astrophys. J.* **698**, 1367–1379 (2009).

14. Maksym, W. P., Ulmer, M. P. & Eracleous, M. A Tidal Disruption Flare in A1689 from an Archival X-ray Survey of Galaxy Clusters. *Astrophys. J.* **722**, 1035–1050 (2010).

15. Zauderer, A. *et al.* The Birth of a Relativistic Outflow in the Unusual γ-ray Transient Swift J164449.3+573451. *Nature,* in press (2011).

16. Gehrels, N. *et al.* The Swift Gamma-Ray Burst Mission. *Astrophys. J.* **611**, 1005–1020 (2004).

17. Barthelmy, S. D. *et al.* The Burst Alert Telescope (BAT) on the SWIFT Midex Mission. *Space Sci. Rev.* **120**, 143–164 (2005).

18. Burrows, D. N. *et al.* The Swift X-Ray Telescope. *Space Sci. Rev.* **120**, 165–195 (2005).

19. Goad, M. R. *et al.* Accurate early positions for Swift GRBs: enhancing X-ray positions with UVOT astrometry. *Astron. Astrophys.* **476**, 1401–1409 (2007).

20. Evans, P. A. *et al.* Methods and results of an automatic analysis of a complete sample of Swift-XRT observations of GRBs. *Mon. Not. R. Astron. Soc.* **397**, 1177–1201 (2009).

21. Levan, A. J. *et al.* An extremely luminous panchromatic outburst from the nucleus of a distant galaxy. *Science* **333**, 199 (2011). `arXiv:1104.3356`.

22. Romano, P. *et al.* Two years of monitoring supergiant fast X-ray transients with Swift. *Mon. Not. R. Astron. Soc.* **410**, 1825–1836 (2011).

23. Bohlin, R. C., Savage, B. D. & Drake, J. F. A survey of interstellar H I from L-alpha absorption measurements. II. *Astrophys. J.* **224**, 132–142 (1978).

24. Grindlay, J. E. Hard X-ray Timing with EXIST. In P. Kaaret, F. K. Lamb, & J. H. Swank (ed.) *X-ray Timing 2003: Rossi and Beyond*, vol. 714 of *American Institute of Physics Conference Series*, 413–422 (2004).

25. Kraft, R. P., Burrows, D. N. & Nousek, J. A. Determination of confidence limits for experiments with low numbers of counts. *Astrophys. J.* **374**, 344–355 (1991).

26. Lodato, G. & Rossi, E. M. Multiband light curves of tidal disruption events. *Mon. Not. R. Astron. Soc.* **410**, 359–367 (2011).

27. Phinney, E. S. Manifestations of a Massive Black Hole in the Galactic Center. In M. Morris (ed.) *The Center of the Galaxy*, vol. 136 of *IAU Symposium*, 543 (1989).

28. Lodato, G., King, A. R. & Pringle, J. E. Stellar disruption by a supermassive black hole: is the light curve really proportional to $t^{-5/3}$? *Mon. Not. R. Astron. Soc.* **392**, 332–340 (2009).

29. Aliu, E. *et al.* VERITAS Observations of the Unusual Extragalactic Transient Swift J164449.3+573451. *Astrophys. J.* in press (2011). `arXiv:1104.3257`.

30. Ghisellini, G. & Tavecchio, F. Canonical high-power blazars. *Mon. Not. R. Astron. Soc.* **397**, 985–1002 (2009).

Supplementary Information is linked to the online version of the paper at www.nature.com/nature.

Acknowledgements We acknowledge support from the following funding agencies: NASA, NSF, and DOE (US); the UK Space Agency; ASI, INAF, and INFN (Italy); the Autonomous Region of Sardinia; MEXT, KEK, and JAXA (Japan); CRI/NRF/MEST (Korea); NSC and Academica Sinica (Taiwan); CEA/Irfu, IN2P3/CNRS, and CNES (France); and the K. A. Wallenberg Foundation, the Swedish Research Council, and the National Space Board (Sweden). We thank the *Swift*, *Fermi*, and *MAXI* operation teams; and we thank Andrew Read for help with the most recent XMM slew data. We gratefully acknowledge the contribution of pre-publication upper limits by the *VERITAS* Collaboration. Finally, we acknowledge the use of public data from the *Swift* and *Fermi* data archives (*http://heasarc.nasa.gov/docs/swift/archive/* and *http://fermi.gsfc.nasa.gov/ssc/*, respectively, as well as data supplied by the UK Swift Science Data Centre at the University of Leicester.

Author Contributions DNB, JAK, and ME composed the text, based on inputs from the other co-authors. Theoretical interpretation was provided by GG, BZ, ME, and PM, with contributions by ADF, SCa, and NG. JAK, VM, KLP, JPO, PR, SCa, APB, VD'E, PE, PAE, and GI processed and analyzed the *Swift* XRT data. TS, JRC, and HAK processed and analyzed the *Swift* BAT data. *Swift* UVOT data were processed and analyzed by AAB, MMC, STH, and FEM.

Ground-based optical/NIR data were obtained with the TNG, BOAO, LOAO, CFHT, UKIRT, and Maidanak Observatory telescopes and were provided, reduced, and analyzed by SCo, PD'A, DF, KYH, MI, HDJ, YJ, Y-BJ, JHK, W-KP, H-IS, GT, YUr, and LAA. *Fermi* LAT data analysis was performed by RC, NO, JSP, and ET. KH, NK, HN, MS, YUe, and RU processed and analyzed the *MAXI* data. ADF provided liason with the *VERITAS* Collaboration. JMG and PG provided analysis of ROSAT archival data, and JO provided analysis of archival XMM data. All authors discussed the results and commented on the manuscript.

Author Information *Swift* data are available from the NASA HEASARC (http://swift.gsfc.nasa.gov/docs/swift/archive/) or from mirror sites in the UK (http://www.swift.ac.uk/swift_portal/archive.php) and Italy (http://swift.asdc.asi.it/). Reprints and permissions information is available at www.nature.com/reprints. The authors have no competing financial interests. Correspondence should be addressed to DNB (burrows@astro.psu.edu).

Figure 1 *Swift* **BAT and XRT light curves for the first three days of observations.** a) BAT light curve (14-195 keV). b) XRT light curve (0.3-10 keV). The horizontal axis is time in days since the first BAT on-board trigger on 28 March 2011. The BAT and XRT count rates track each other closely, with episodes of bright flaring (up to 200 mCrabs in the BAT) in the first few days after the first BAT trigger on 28 March 2011. The source brightness then dropped dramatically, with an average BAT count rate of 0.0020 ± 0.0005 counts cm^{-2} s^{-1} between 2 April 2011 and 18 April 2011. Data gaps are caused by times when the source was not being observed. Error bars are one standard deviation.

Figure 2 ***Swift*** **XRT light curve of Sw J1644+57 for the first 7 weeks of observations.** a) Historical 3σ X-ray flux upper limits from the direction of Sw J1644+57, obtained by sky monitors and serendipitous observations over the last 20 years. The time axis for this panel is in years before the BAT on-board trigger on 28 March 2011. The horizontal bars on each upper limit indicate the time interval over which they were calculated, and are placed at the value of the 3σ upper limit. All flux limits are calculated for the 1–10 keV band. (The BAT upper limit measured in its native energy band is about 3 orders of magnitude lower than the peak flux measured by the BAT during the early flares). b) XRT light curve in the 1–10 keV band. The X-ray events were summed into time bins containing 200 counts per bin and count rates were calculated for each time bin. Time-dependent spectral fits were used to convert count rates to absorption-corrected fluxes in the 1–10 keV band. The right-hand axis gives the conversion to luminosity of the source, assuming isotropic radiation and using $\mathrm{H_0} = 71$ km s^{-1}, $\Omega_\mathrm{m} = 0.27$, and $\Omega_\Lambda = 0.73$. Following nearly 3 days of intense flaring with peak fluxes over 10^{-9} erg cm^{-2} s^{-1} and isotropic luminosities of $\sim 10^{48}$ erg s^{-1}, Sw J1644+57 decayed over several days to a flux of about 5×10^{-11} erg cm^{-2} s^{-1}, then rose rapidly to $\sim 2 \times 10^{-10}$ erg cm^{-2} s^{-1} for about a week. It has been gradually fading since. Details of the upper limits and XRT light curve are given in the Supplementary Information section 1. Vertical error bars are one standard deviation. Time bin widths are smaller than the line width for the vertical error bars.

Figure 3 The Spectral Energy Distribution of Sw J1644+57. The green data points are from the early bright flaring phase; cyan data points are from the low state at 4.5 days; black data points are from roughly 8 days after the first BAT trigger. The near-IR (NIR) fluxes were dereddened with $A_V = 4.5$, and the X-ray data were corrected for absorption by $N_H = 2 \times 10^{22}$ cm^{-2}. Upper limits from the *Fermi* LAT (2×10^{23} Hz) and from *VERITAS*[29] (10^{26} Hz) are also shown. The red curve is a blazar jet model[30] dominated by synchrotron emission, fit to the spectral energy distribution of the brightest flares. On the low frequency side, the steep slope between the NIR and X-ray bands requires suppression of low-energy electrons, which would otherwise overproduce the NIR flux. This requires a particle-starved, magnetically-dominated jet. On the high frequency side, the LAT (95%) and *VERITAS* (99%) upper limits require that the self-Compton component (red dashed line) is suppressed by γ-γ pair production, which limits the bulk Lorentz factor in the X-ray emitting region to be $\Gamma \lesssim 20$. The model includes a disk/corona component from the accretion disk (black dotted curve), but the flux is dominated at all frequencies by the synchrotron component from the jet. The blue curve shows the corresponding model in the low X-ray flux state. The kink in the X-ray spectrum in the low and intermediate flux states suggests that a possible additional component may be required; it would have to be very narrow, and its origin is unclear. Further details, including model parameters and two alternative models, are presented in the Supplementary Information section 2.

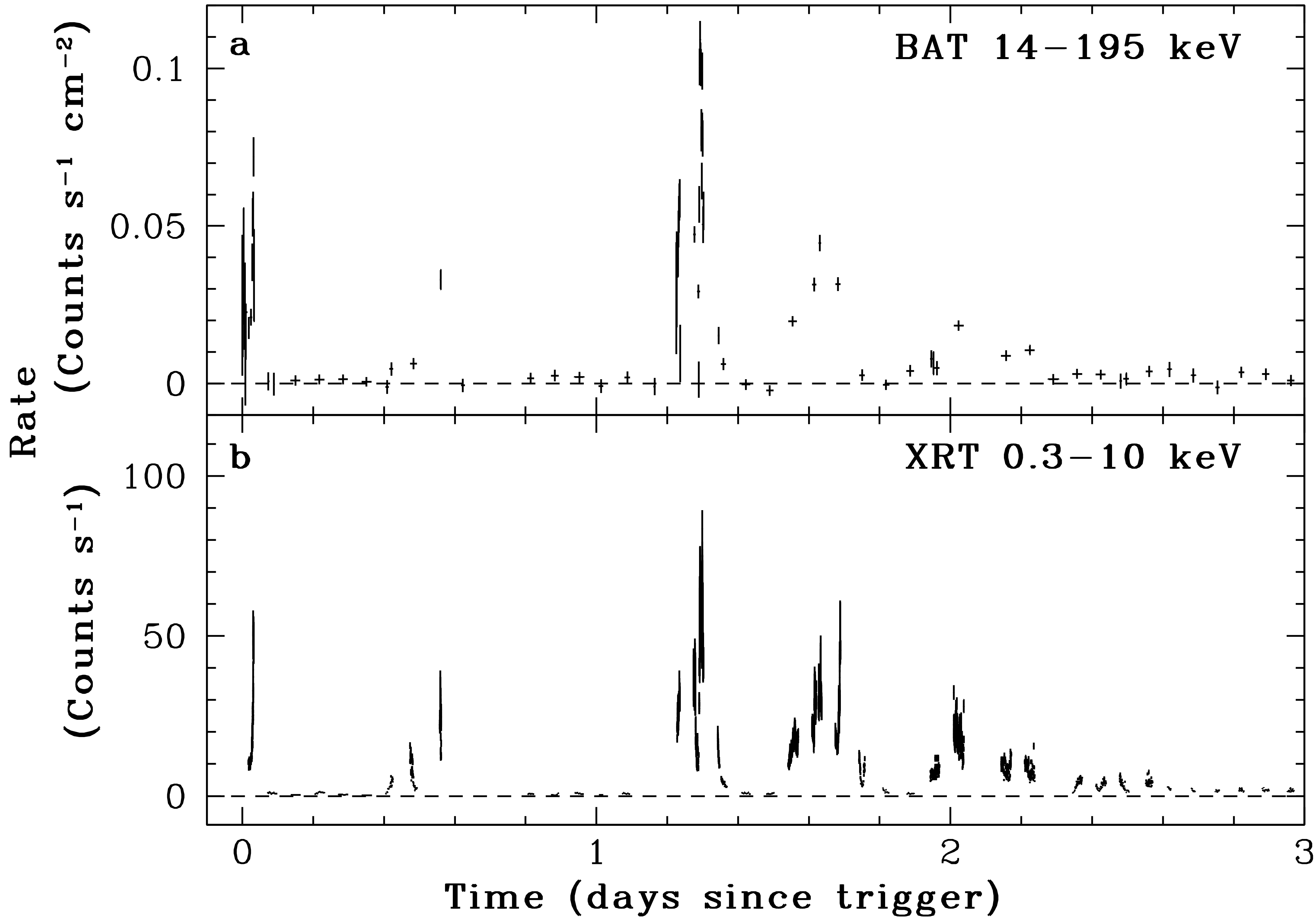

a
BAT 14−195 keV
b
XRT 0.3−10 keV
Rate
(Counts s⁻¹ cm⁻²)
(Counts s⁻¹)
0.1
0.05
0
100
50
0
1
2
3
Time (days since trigger)

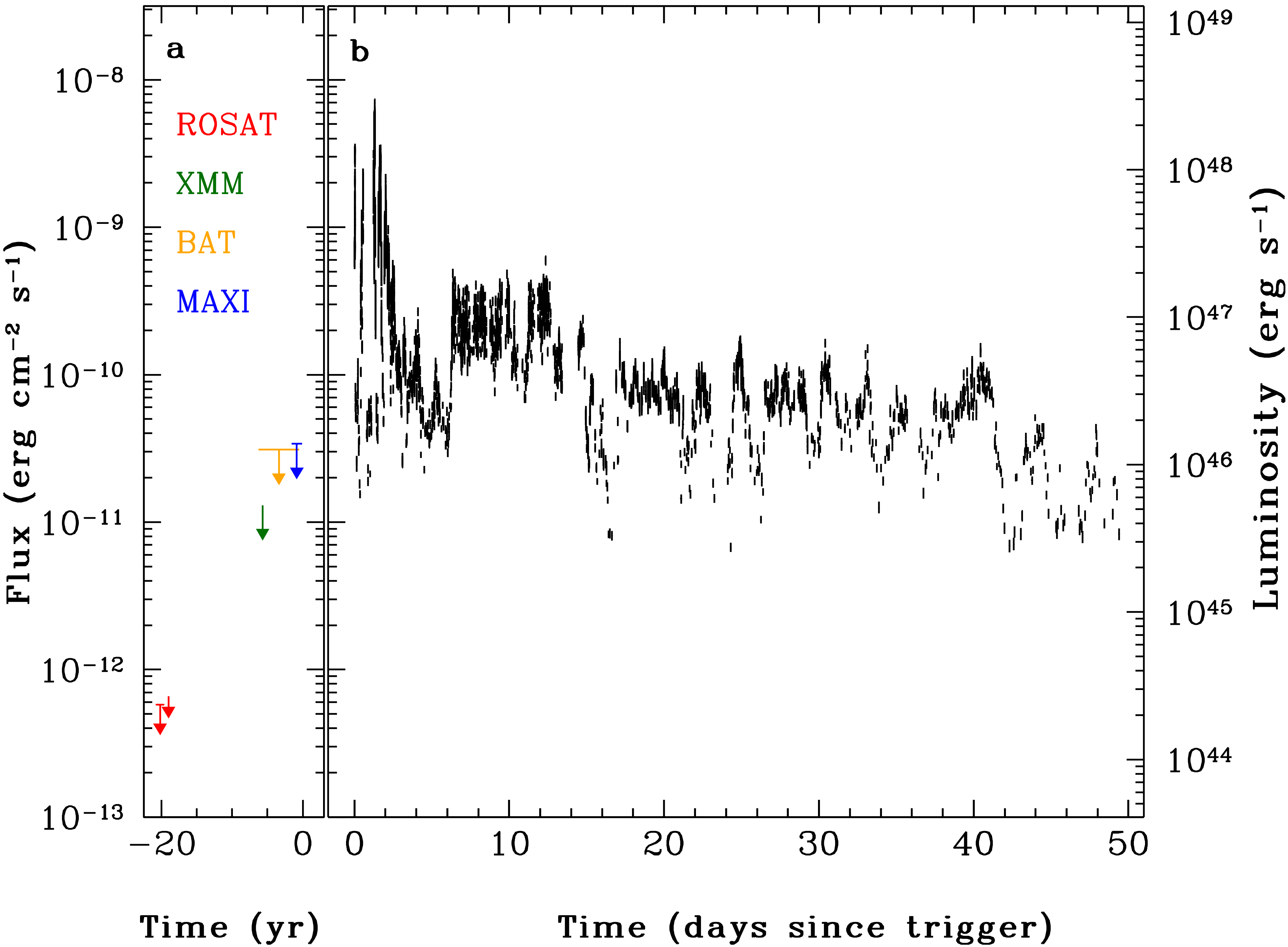
a
b
ROSAT
XMM
BAT
MAXI
10^{-8}
10^{-9}
10^{-10}
10^{-11}
10^{-12}
10^{-13}
Flux (erg cm^{-2} s^{-1})
10^{49}
10^{48}
10^{47}
10^{46}
10^{45}
10^{44}
Luminosity (erg s^{-1})
−20
0
0
10
20
30
40
50
Time (yr)
Time (days since trigger)

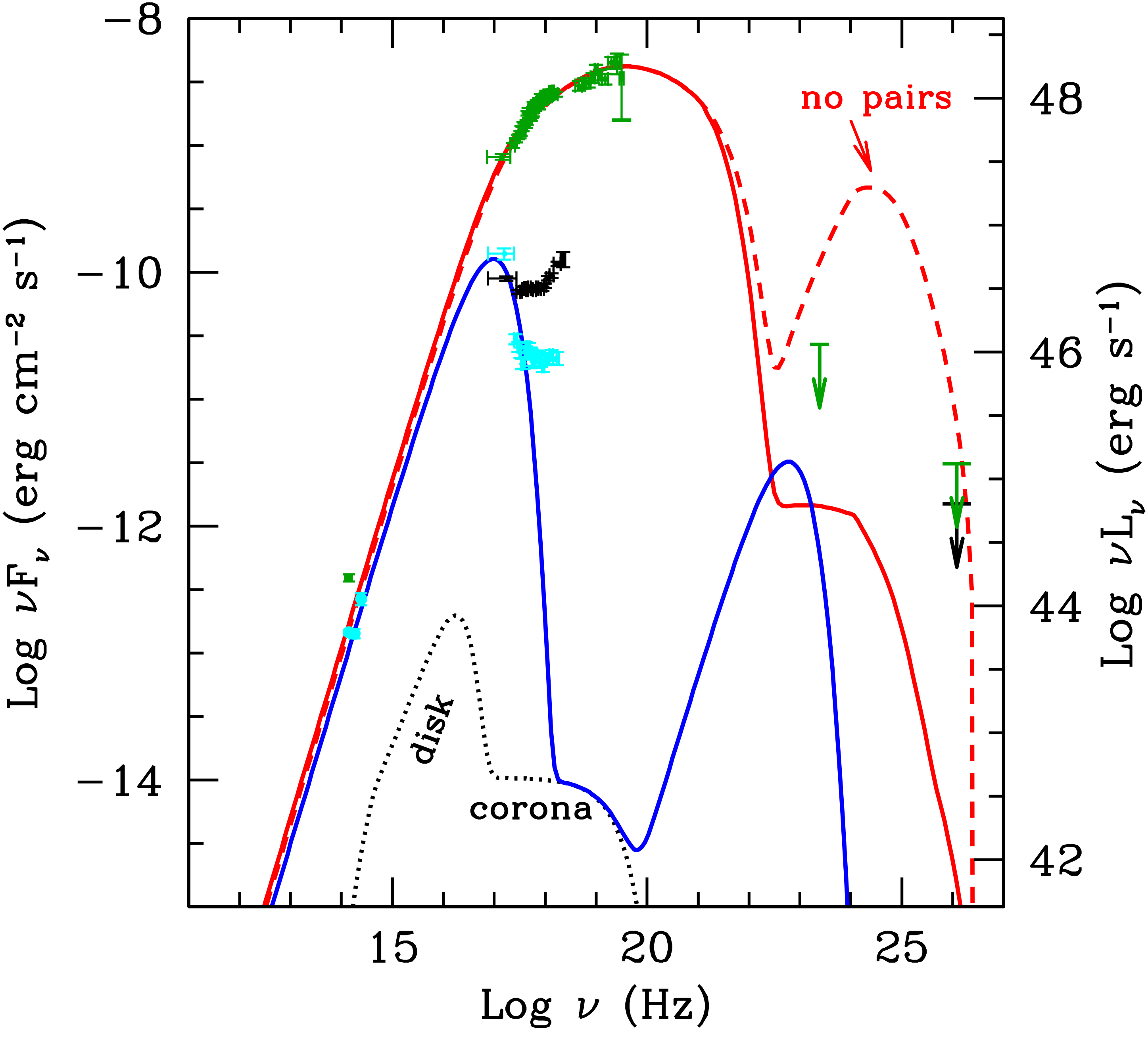

Log νF_ν (erg cm^{-2} s^{-1})
Log νL_ν (erg s^{-1})
Log ν (Hz)
−8
−10
−12
−14
48
46
44
42
15
20
25
no pairs
disk
corona